



Queensland University of Technology
Brisbane Australia

This may be the author's version of a work that was submitted/accepted for publication in the following source:

[Randiligama, S. M. Chathurangi M., Thambiratnam, David P., Chan, Tommy H. T., & Fawzia, Sabrina](#)

(2021)

Damage assessment in hyperbolic cooling towers using mode shape curvature and artificial neural networks.

Engineering Failure Analysis, 129, Article number: 105728.

This file was downloaded from: <https://eprints.qut.edu.au/226356/>

© 2021 Elsevier Ltd.

This work is covered by copyright. Unless the document is being made available under a Creative Commons Licence, you must assume that re-use is limited to personal use and that permission from the copyright owner must be obtained for all other uses. If the document is available under a Creative Commons License (or other specified license) then refer to the Licence for details of permitted re-use. It is a condition of access that users recognise and abide by the legal requirements associated with these rights. If you believe that this work infringes copyright please provide details by email to qut.copyright@qut.edu.au

License: Creative Commons: Attribution-Noncommercial-No Derivative Works 2.5

Notice: *Please note that this document may not be the Version of Record (i.e. published version) of the work. Author manuscript versions (as Submitted for peer review or as Accepted for publication after peer review) can be identified by an absence of publisher branding and/or typeset appearance. If there is any doubt, please refer to the published source.*

<https://doi.org/10.1016/j.engfailanal.2021.105728>

Damage Assessment in Hyperbolic Cooling Towers Using Mode Shape Curvature and Artificial Neural Networks

S. M. Chaturangi M. Randiligama^{a,*}, David P. Thambiratnam^a, Tommy H. T. Chan^a, Sabrina Fawzia^a

^a *Queensland University of Technology (QUT), 2 George St, Brisbane, QLD 4001, Australia*

Abstract

Hyperbolic cooling towers are large thin shell reinforced concrete structures that are used to remove the heat from wastewater and transfer it to the atmosphere using the process of evaporation. During its long service life, a cooling tower can experience damage due to the large temperature variations, environmental degradation, or random actions such as impacts or earthquakes. Such a damage can develop over time and result in the sudden collapse of the cooling tower. To ensure that a cooling tower operates safely and efficiently at all times, it is important to monitor its structural health. In this context, structural health monitoring based on the vibration characteristics of the structure, has emerged as a useful method to detect and locate damage in structures. Hyperbolic cooling towers, due to their particular shape, exhibit rather complex vibration characteristics that do not suit the traditional vibration-based damage detection techniques. This paper develops and applies a damage assessment method using the absolute changes in mode shape curvature (ACMSC) in conjunction with Artificial Neural Networks (ANNs) to detect, locate, and quantify damage in hyperbolic cooling towers. ANN is a machine learning technique that can predict behavioural patterns using a set of data samples and finds use in the damage quantification process. The proposed method for detecting and locating damage is experimentally validated and demonstrated its capability to accurately detect and locate damage. A feed-forward network having one hidden layer with Bayesian algorithm is used to train the artificial neural network. Damage indices calculated from noise polluted mode shape data are used to train the network. The trained network is then used to successfully assess the unknown damage severities in the cooling tower. The outcomes of this paper will enable early warning of damages in the cooling towers and will help towards their safe operation.

Keywords: Hyperbolic Cooling Tower; Vibration Characteristics; Structural Health Monitoring; Artificial Neural Network; Damage Quantification; Absolute Change in Mode Shape Curvature Method

* Corresponding author: S.M. Chaturangi M. Randiligama, Queensland University of Technology, 2 George St, Brisbane, QLD 4001, Australia.
Email: charhurangi.mudiyanselage@hdr.qut.edu.au

Nomenclature

The following symbols are used in this paper

ACMSC	Absolute change in mode shape curvature	SHM	Structural health monitoring
ANN	Artificial Neural Network	U_1	Radial component
DIs	Damage indices	U_3	Vertical component
FEM	Finite element model	VBDD	Vibration based damage detection
h	Length of the element	$\phi_{j, i}$	Magnitude of the mode shape of i^{th} vibration mode at j^{th} location
MSE	Mean square error	γ_x^ϕ	Random number with mean of zero and variance of 1
R	Regression	ρ_x^ϕ	Random noise level

32

33 1. Introduction

34 Hyperbolic cooling towers are large, reinforced concrete structures which are constructed to have
35 long service lives. Their fundamental task is to eliminate the waste heat from the water and transfer it
36 to the atmosphere [1]. Hyperbolic cooling towers are doubly curved thin-walled shell structures that
37 can better withstand external pressure (than straight towers) [2]. During the service life of a cooling
38 tower, sudden damage or collapse can occur due to structural deterioration, random actions, and
39 environmental effects. It is therefore beneficial to examine the structural health of all important and
40 especially large structures on a regular basis to ensure that they operate safely. Since most of the
41 hyperbolic cooling towers are very tall and large in diameter, visual inspection can be very difficult,
42 especially in the interior of the towers. Today, most inspections and assessments are done using non-
43 destructive tests to detect the onset of damage and carry out appropriate retrofits to prevent the structure
44 from collapse. [3], [4]. In this context, structural health monitoring (SHM) based on vibration
45 characteristics of the structure has emerged as a useful technique. The principle of this technique is
46 that the damage in a structure causes a change in its vibration properties, and this change can be used

47 to detect damages in the structure. Vibration-based damage detection (VBDD) techniques are
48 categorized as global methods [5]. They are cost-effective and comparatively easy to apply. Over the
49 last few decades, mode shapes [6] and mode shape derivatives [7] have been used as damage detection
50 indicators. Mode shape curvature is the second derivative of mode shape, and it has a direct relationship
51 with bending strains in beams, plates, and shells [8]. Absolute change in mode shape curvature
52 (ACMSC) can hence be an effective tool for detecting and locating structural damage.

53 Dynamic behaviour of a structure depends on the structure type, and hence damage detection
54 methods developed for one structure type are normally not be applicable to other structure types.
55 Hyperbolic cooling towers due to their unique shape, have rather complex vibration characteristics. It
56 is thus necessary to develop an appropriate vibration-based damage detection method to detect, locate,
57 and quantify the damage in them. To address this a coupled method associated with ACMSC was
58 developed to successfully detect and locate damage in hyperbolic cooling towers, as presented in [9].
59 Quantifying the damage or predicting damage severity is a more challenging task than that of detecting
60 and locating the damage and it is usually not within the capability of vibration-based damage detection
61 methods. Existing numerical methods used for damage quantification in beams [10] and trusses [11]
62 have some drawbacks. They are not generic but are specific for a particular structure and may not be
63 capable of quantifying the damages in complex structures. There are few references in the literature
64 on damage quantification in bridge structures using the combination of vibration characteristics and
65 ANN [12], [13]. This present paper develops and applies ANN techniques, in conjunction with
66 ACMSC method to detect, locate and quantify damage in hyperbolic cooling towers and thus complete
67 the task of damage assessment in these types of structures.

68 ANN, which imitates the mechanism of the human brain is introduced as a smart and efficient
69 tool to assess (locate and quantify) damage in cooling towers. ANN comprises of a large number of
70 neurons which are simple processing units [14]. It can capture complex relationships between input
71 and output through the process of learning, self-organizing, and auto improving [15]. A properly

72 trained network is capable of predicting the accurate output from unknown input data which are
 73 inconsistent, noise polluted, and uncertain [16]. The method proposed in this paper is verified for a
 74 full-scale hyperbolic cooling tower for a range of damage scenarios. Further, its capability of damage
 75 quantification under field conditions is tested by adding white Gaussian noise to the input data in the
 76 numerical simulations. Results confirm the accuracy of the proposed method to detect, locate and
 77 quantify method in hyperbolic cooling towers and the outcomes of this paper will enable the safer
 78 operation of these large structures.

79 **2. Methodology**

80 *2.1 Vibration based damage detection method*

81 Hyperbolic cooling towers have complicated vibration mode shapes due to their geometrical
 82 shape. Preliminary studies indicate that the radial (U1) and vertical (U3) components of mode shapes
 83 in general provide the greater contribution for damage detection in hyperbolic cooling towers [9].
 84 Therefore, instead of the resultant modes, mode shape components corresponding to maximum
 85 effective mass values are chosen for the process of damage detection considering the first three global
 86 modes [9]. The finite element model (FEM) of the cooling tower structure has two modes with the
 87 same frequency and similar mode shape, due to its symmetry. Therefore, the first three global modes
 88 represent the 1st, 3rd, and 5th mode shapes in general.

89 According to the Pandey et al. 1991[17], the mode shape curvature method was used to locate
 90 damage in cantilever and simply supported beams. Mode shape curvature can be determined from
 91 displacement mode shapes as in Equation 1 using the central difference approximation.

$$92 \quad \phi_{j,i}'' = \frac{\phi_{j-1,i} - 2\phi_{j,i} + \phi_{j+1,i}}{h^2} \quad (1)$$

93 where h is the distance between two nodes and $\phi_{j,i}$ is the mode shape of the jth element for ith mode.

94 As observed previously [9], the highest peak in the absolute change in mode shape curvature (ACMSC)

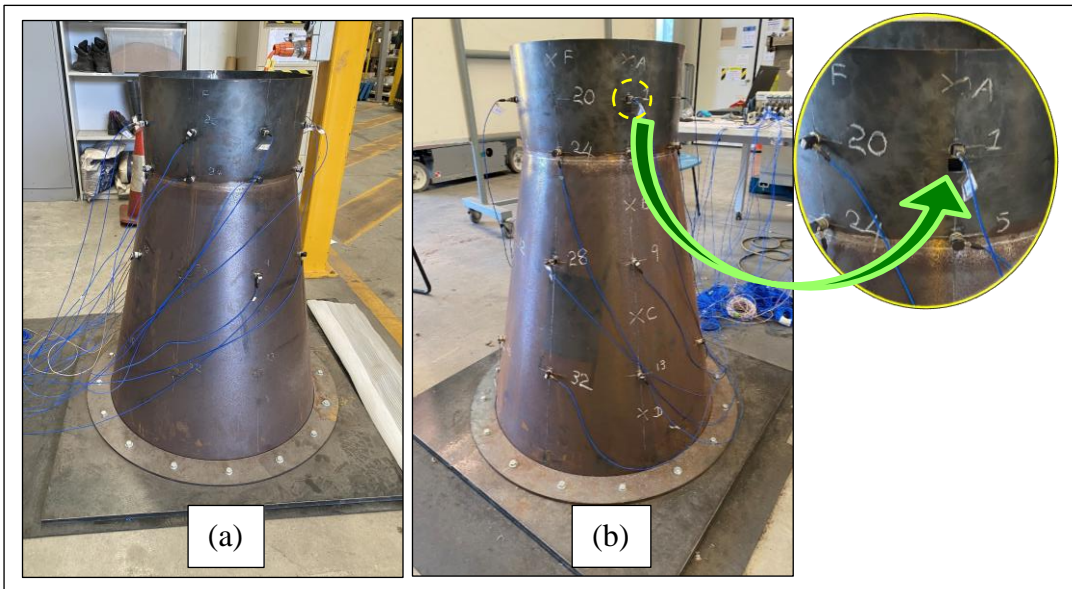
95 between damage and intact states as shown in Equation 2 indicates the location of the damage in the
96 hyperbolic cooling tower.

$$97 \quad \mathbf{DI} = \Delta\phi_{j,i}'' = \left[\frac{\phi_{j-1,i} - 2\phi_{j,i} + \phi_{j+1,i}}{h^2} \right]^d - \left[\frac{\phi_{j-1,i} - 2\phi_{j,i} + \phi_{j+1,i}}{h^2} \right]^u \quad (2)$$

98 In the above equation superscripts u and d denote the undamaged and damaged states, respectively.

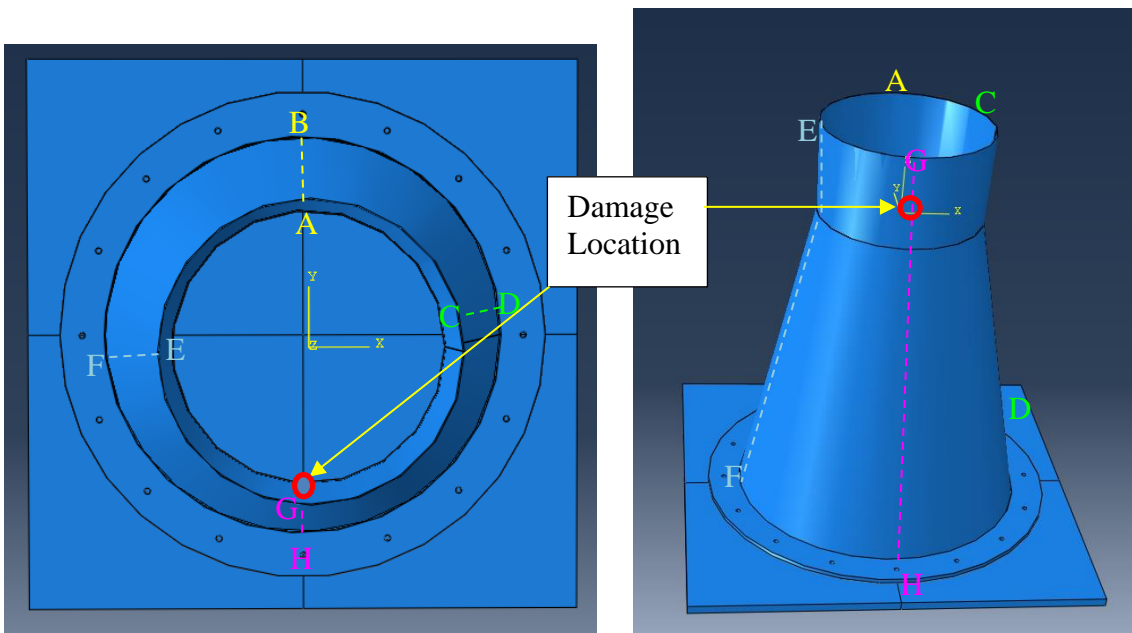
99 The above procedure was validated experimentally, and details are provided in [9]. For the
100 completeness of this paper, a brief description of the validation is presented below.

101 Feasibility of the proposed method was verified using the results from experimental testing of
102 laboratory scale cooling tower models, shown in Fig.1. The cooling tower models were made from
103 general steel. Free vibration tests were carried out on the intact and damaged models to obtain the
104 natural frequencies and mode shapes and were used to validate the proposed method under laboratory
105 conditions. In practical situations, mode shape data are not measured directly, but are obtained from
106 measured acceleration data. Damage was introduced by cutting a small hole in the upper section of the
107 cooling tower model, as shown in Fig.1.



119 Fig.1. (a) Experimental cooling tower model with accelerometer arrangement (b) Damage at the
120 upper section of the cooling tower model

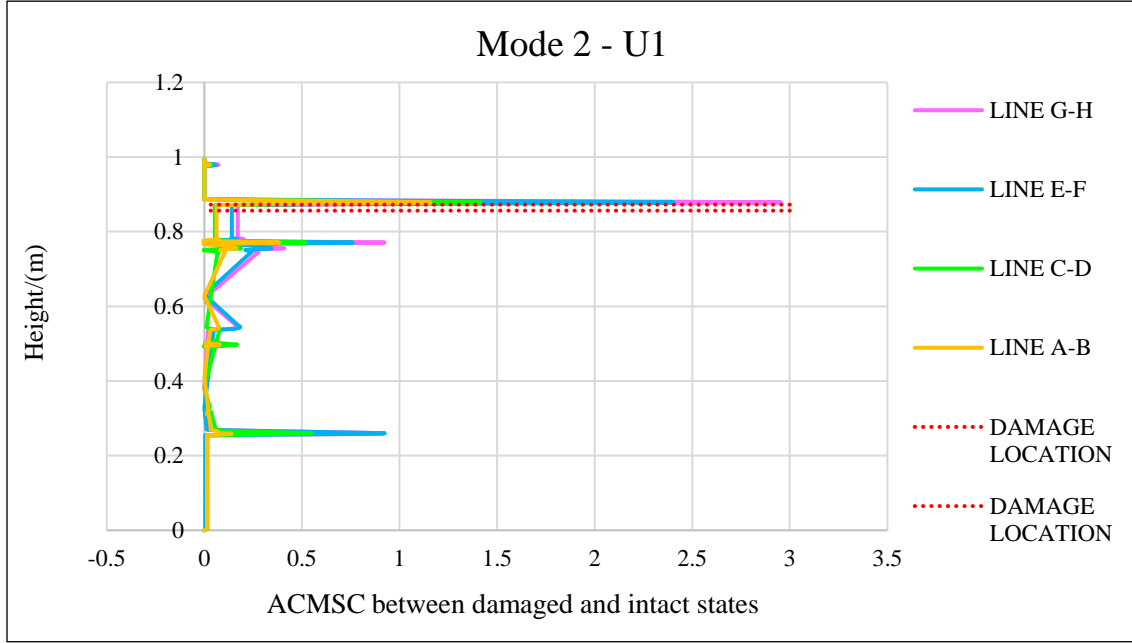
121 A finite element model (FEM) of the experimental cooling tower was simulated in ABAQUS
 122 finite element modelling software package and validated by comparing the natural frequencies of the
 123 numerical and experimental models. Dominant effective mass values were extracted from the
 124 undamaged finite element model. Mode and mode shape components corresponding to maximum
 125 effective mass values were used to calculate Damage Indices (DIs), plot the DIs along a few vertical
 126 cross-sections to accurately determine the damage location. Lines A-B, C-D, E-F and G-H in Fig. 2
 127 indicate the different vertical cross-sections of the cooling tower model considered in the damage
 128 detection process. Line G-H is very close to the damage location while the distance to the damage
 129 location gradually increases for lines E-F, C-D, and A-B. The two lines of “Damage Location” in
 130 legend of Fig. 3 indicate the starting point and ending point of the damage area. It can be seen from
 131 Fig. 3 that the damage around the upper section of the cooling tower model is precisely detected by
 132 the proposed procedure which can hence be considered as validated.



140 Fig.2. (a) Plan view (b) Front view of selected nodal paths

141 The applicability of the proposed damage detection method was illustrated using the full-scale
 142 Mülheim-Kärlich hyperbolic cooling tower in Germany [18]. A full-scale finite element model of this
 143 cooling tower was developed using ABAQUS finite element modelling software. The height of the

144 Mülheim-Kärlich cooling tower is 162 m. The throat, top and base diameters are 65.3 m, 68 m, and
 145 117 m, respectively, while the thickness of the tower is 0.24 m. The throat is located 37 m above the
 146 base of the tower. As mentioned in the literature [19], unit weight, Poisson's ratio and Young's
 147 modulus of concrete were considered as 25kN/m³, 0.2, and 39GPa, respectively.



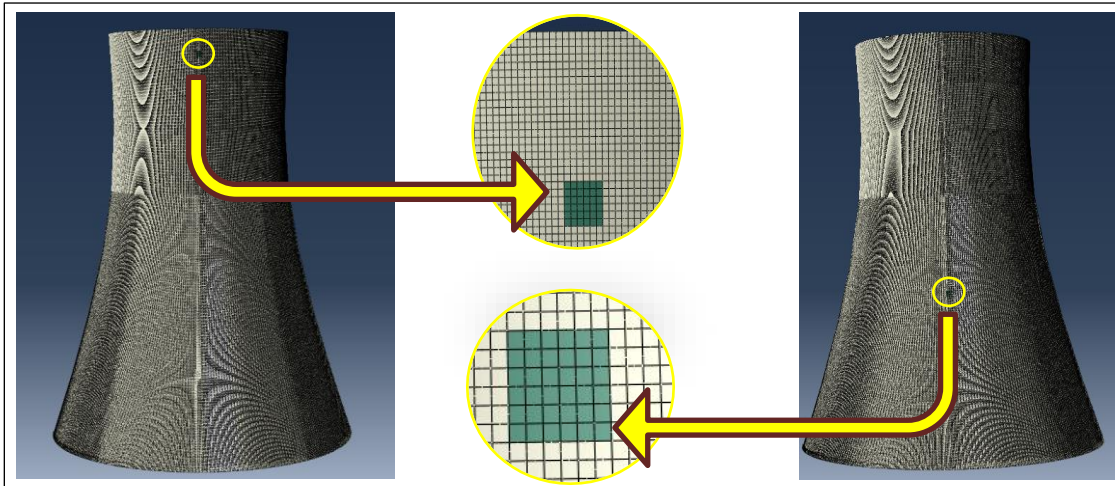
161 Fig.3. Locating damages at upper section of the cooling tower using dominant mode shape
 162 component (Mode 2 -U1)

163 Table 1. Selection of mode shape and mode shape component

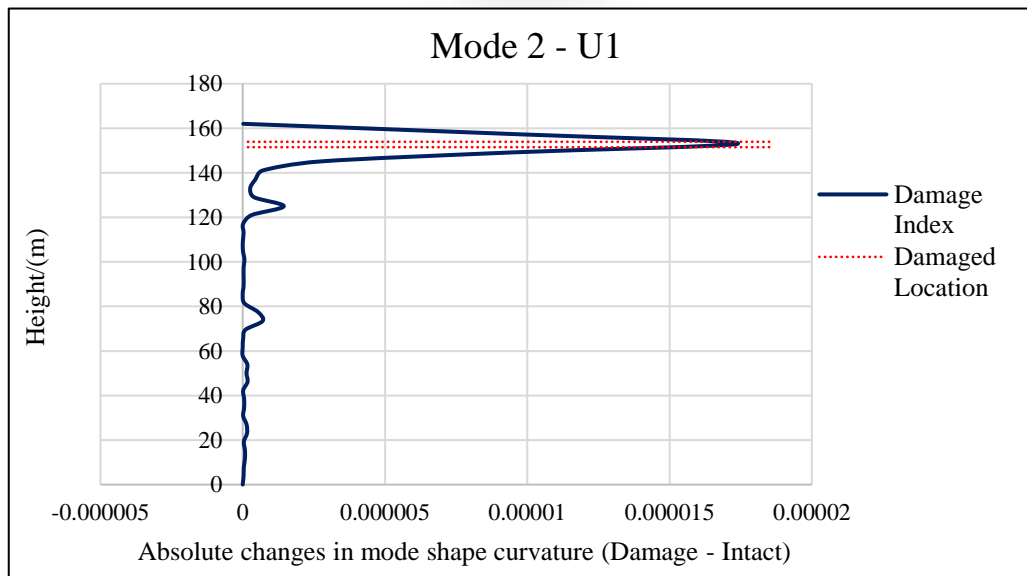
Tower	Global Mode	Effective mass of U1 direction	Effective mass of U3 direction	Maximum effective mass	Selected mode shape and component
Mülheim-Kärlich	1	1.36E-12	1.68E-13		
	2	5.41E-10	1.47E-10	5.41E-10	Mode 2 – U1
	3	2.85E-10	5.32E-10		

164
 165 Two damage cases, one at a time, were simulated by reducing the 10% of the Young's modulus
 166 at a small area in the upper section and the bottom section of the cooling tower, as shown in Fig. 4 to
 167 demonstrate the ability of proposed damage detection method. As described above, effective masses
 168 corresponding to first three global modes (1st, 3rd, and 5th mode shapes in general) are extracted from

169 the intact finite model, as shown in Table 1. The mode and mode shape component (Mode 2 - U1)
 170 corresponding to maximum effective mass values is selected for the damage detection process. Figs.5
 171 and 6 clearly show the significant increase of DIs at the damage locations in the upper and lower
 172 sections of the hyperbolic cooling tower.



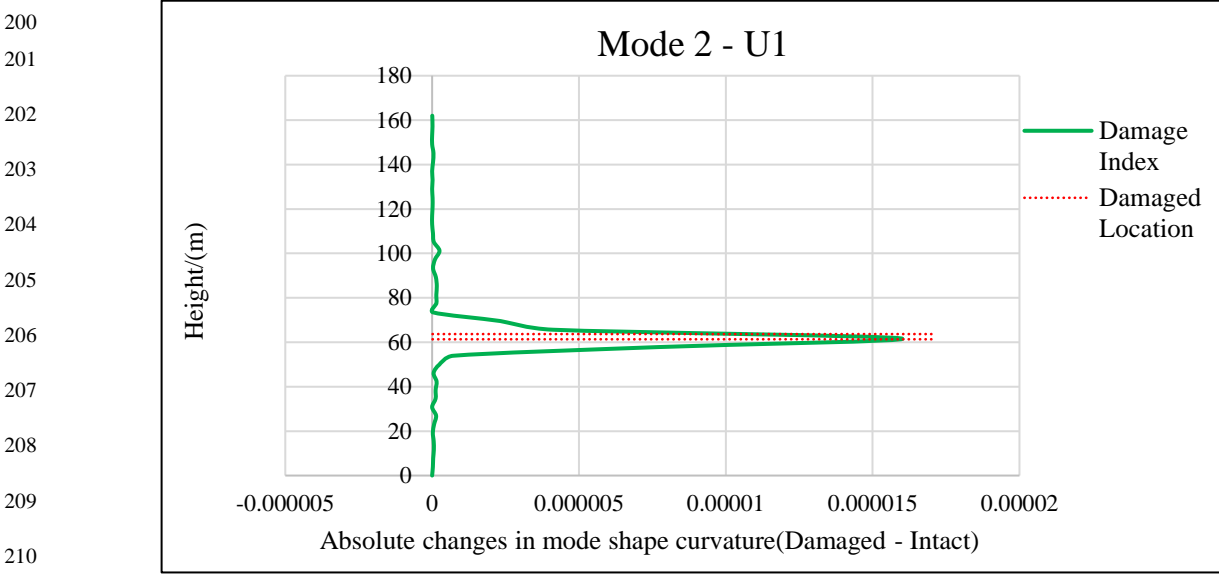
182 Fig.4. Two damage scenarios of hyperbolic cooling tower



190 Fig. 5. Results of locating damage between the neck and the upper section of Mülheim-Kärlich
 191 cooling tower

192 These results demonstrate that the proposed method is able to detect and locate damage in
 193 hyperbolic cooling towers as shown in Figs 5 and 6. Figs. 7,8 and 9 show the plots of the damage index
 194 (ACMSC) at three different locations for different damage intensities. It is evident from these figures

195 that the intensity of damage at a location is proportional to the peak of the damage index at that
 196 location. This paper therefore explores the use of regression analysis to quantify damage and then due
 197 to its limitation, it develops and applies Artificial Neural Networks (ANNs) to extend the damage
 198 assessment procedure to quantify (or predict damage severity) under field conditions and thereby
 199 complete damage assessment in hyperbolic cooling towers.



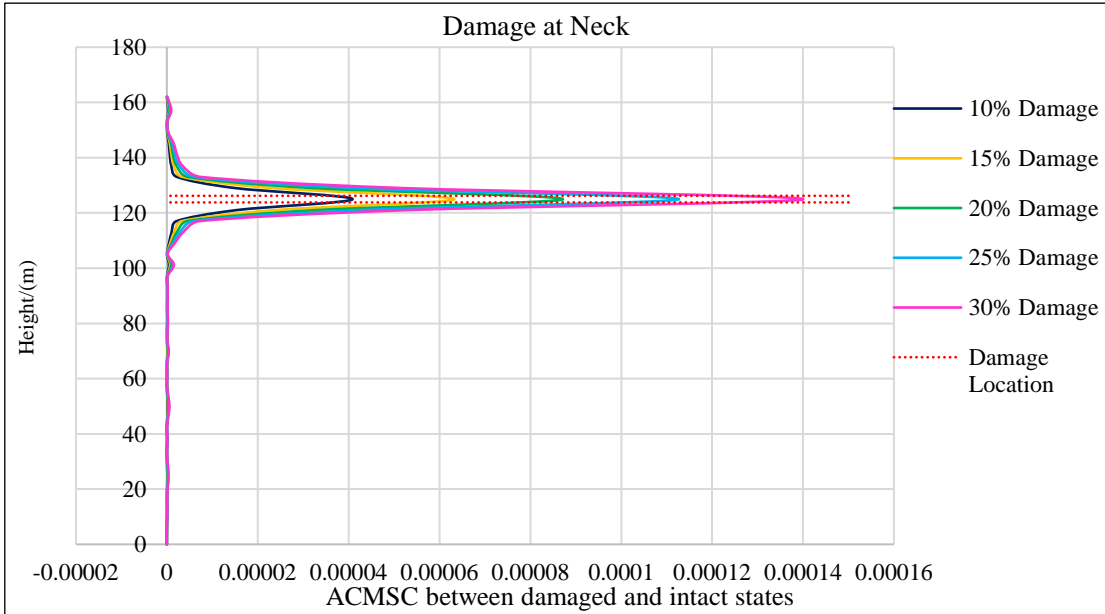
211 Fig. 6. Results of locating damage between the neck and the bottom section of Mülheim-Kärlich
 212 cooling tower

213 3. Damage quantification

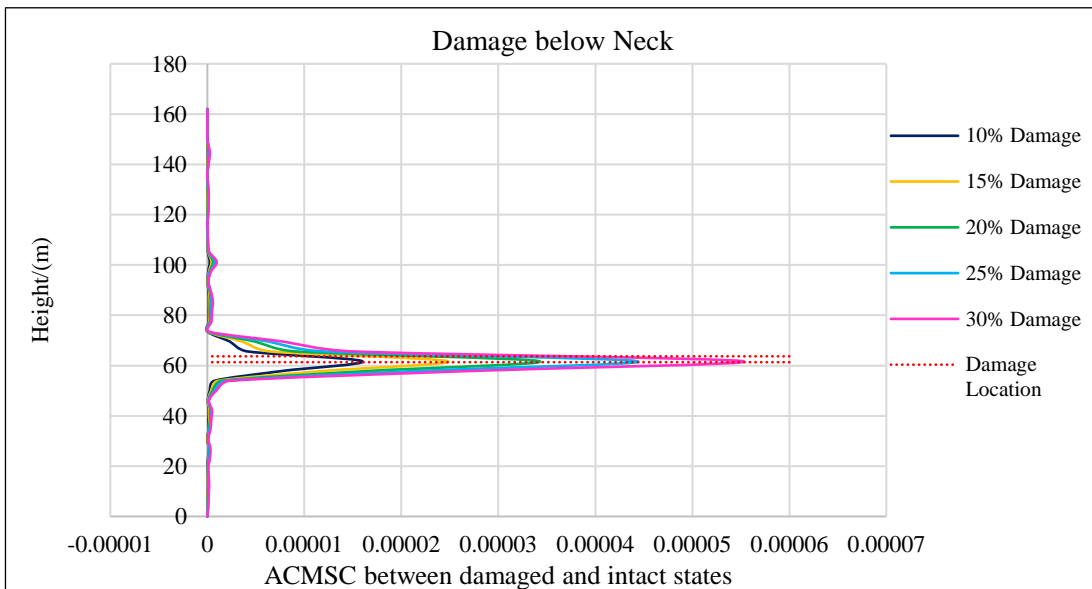
214 3.1 Damage quantification in hyperbolic cooling towers using linear regression

215 The Mülheim-Kärlich cooling tower mentioned earlier was selected to test the proposed damage
 216 quantification method. As categorized by the Rytter [20], quantifying the severity of the damage is the
 217 third level of damage detection in a SHM system. Compared to detecting and locating damage,
 218 quantification of damage is quite a challenging task. Most of the procedures for damage quantification
 219 are not generic but treat specific simple structures such as beams [10] and trusses [11]. These
 220 techniques may not be pertinent for damage quantification in complex structures. To address this issue,
 221 this paper first tried using ACMSC based damage indices (DIs) to quantify damage in cooling towers.

222 As shown in the Figs. 7, 8 and 9, the ACMSC based DIs are plotted along the height of the
 223 cooling tower for different damage severities of 10%,15%,20%,25% and 30% (or stiffness reductions).
 224 The damage is represented by reducing the Young's modulus of elements in a small area at the
 225 particular damage location.

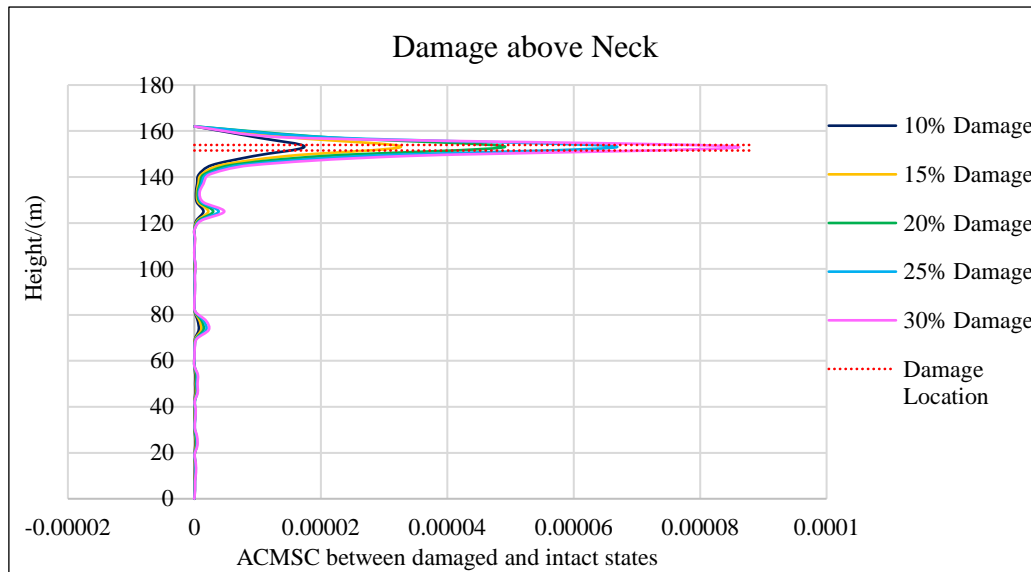


234 Fig. 7. Plots of DIs based on ACMSC for 10%, 15%, 20%, 25% and 30% damage (stiffness
 235 reduction) at the neck of the Mülheim-Kärlich cooling tower



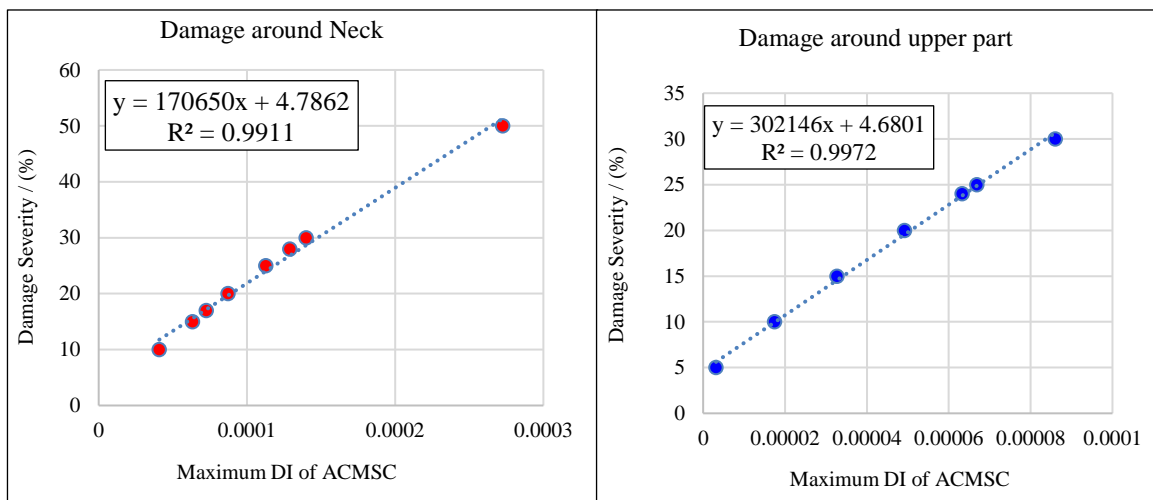
243 Fig. 8. Plots of DIs based on ACMSC for 10%, 15%, 20%, 25% and 30% damage (stiffness
 244 reduction) between the neck and base of the Mülheim-Kärlich cooling tower

245
246
247
248
249
250
251
252

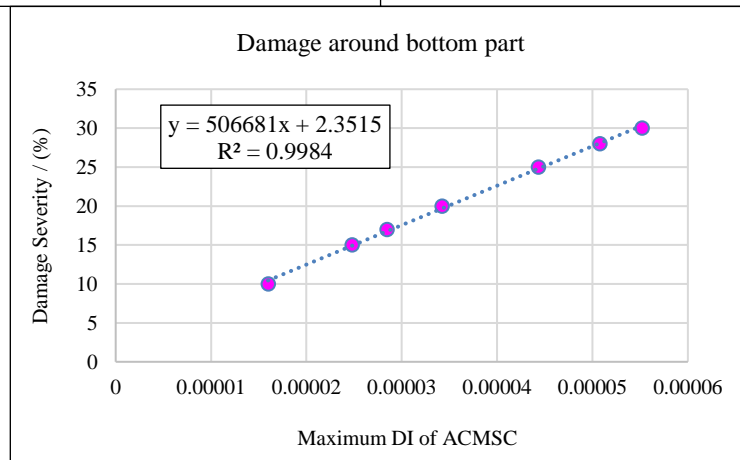


253 Fig. 9. Plots of DIs based on ACMSC for 10%, 15%, 20%, 25% and 30% damage between the neck
254 and top of the Mülheim-Kärlich cooling tower

255
256
257
258
259
260



261
262
263
264
265



266 Fig. 10. Plot of maximum DI values of ACMSCs vs percentage stiffness reduction in (a) neck (b)
267 upper part and (c) lower part of Mülheim-Kärlich cooling tower

268 As seen from these Figures the maximum values of the DIs, at a particular damage location
 269 seem to vary linearly with the severity of the damage. Linear regression analysis was therefore used to
 270 develop an the equation for damage quantification in hyperbolic cooling towers. A set of equations
 271 was developed for the three different locations, as shown in Figs. 10 (a),(b) and (c). In this process,
 272 the damaged location has to be determined first using ACMSC method and then maximum DI value
 273 of ACMSC in that nodal path can be applied to the relevant equation to calculate damage severity as
 274 shown in Table 2. These equations unfortunately are not capable of quantifying damage when DIs are
 275 calculated in the presence of noise.

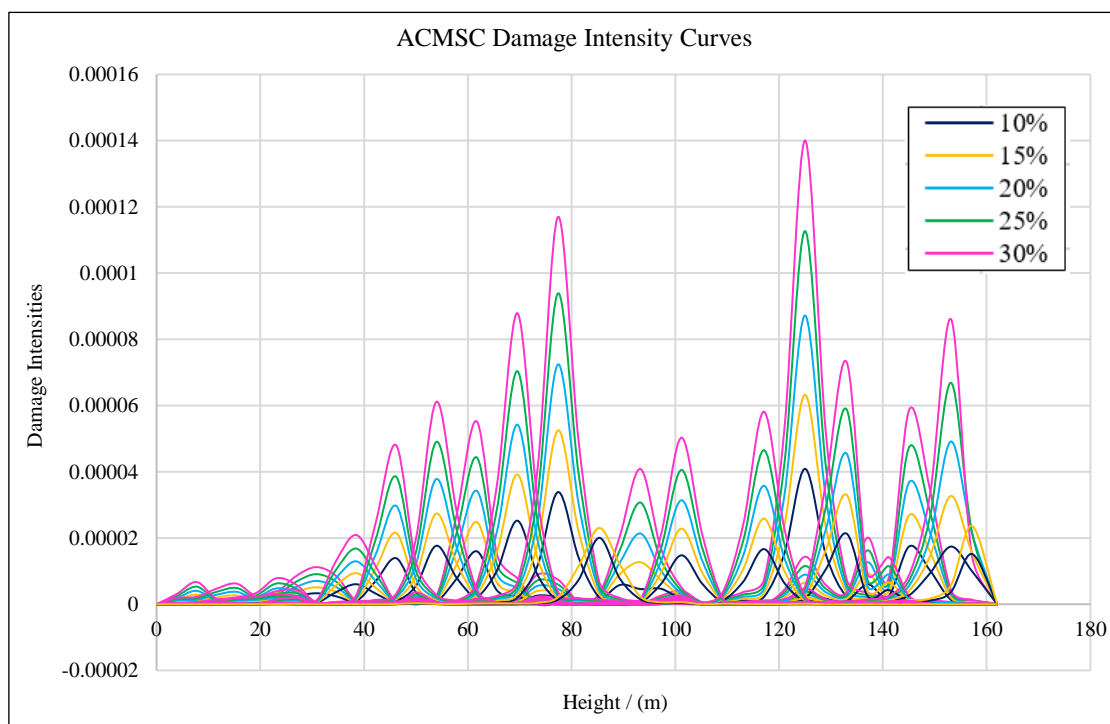
276 Table 2. Calculation of damage severity using equations

Location	Absolute damage severity	Results obtained from equations	Variation
Damage around neck of the tower	12.5%	13.65%	-1.15%
	22.5%	21.80%	0.70%
	35%	33.70%	1.30%
Damage around neck and upper section of the tower	13%	12.67%	0.33%
	33%	34.39%	-1.39%
	40%	43.80%	-3.80%
Damage around neck and bottom section of the tower	12.5%	12.64%	-0.14%
	22.5%	22.21%	0.29%
	35%	36.28%	-1.28%

277 Table 2 compares the predicted damage severities at the 3 locations obtained from these
 278 equations with the actual damage severities at these locations. It is evident that the errors are quite
 279 small making the results quite acceptable.
 280

281

282 Fig. 11 shows the plots of the ACMSC based DIs for 20 damage scenarios along the height of
283 the Mülheim-Kärlich cooling tower for 10%,15%, 20%, 25% and 30% damage severities. As shown
284 there, the peak value is location specific. The peak values of DIs curves can be different for two similar
285 damage intensities at different locations. Therefore, these patterns can cause problems when the
286 location and intensity of the damage are not known. To overcome this issue, most researchers have
287 commonly used ANN, generic algorithm, and computational intelligence techniques to quantify the
288 damage severities of the structure [21], [22]. To address the problems with using equations to quantify
289 damage, this paper develops and applies ANNs. These ANNs are trained to detect, locate, and quantify
290 damage in hyperbolic cooling towers using the vibration characteristics (mode shapes) of the cooling
291 tower.



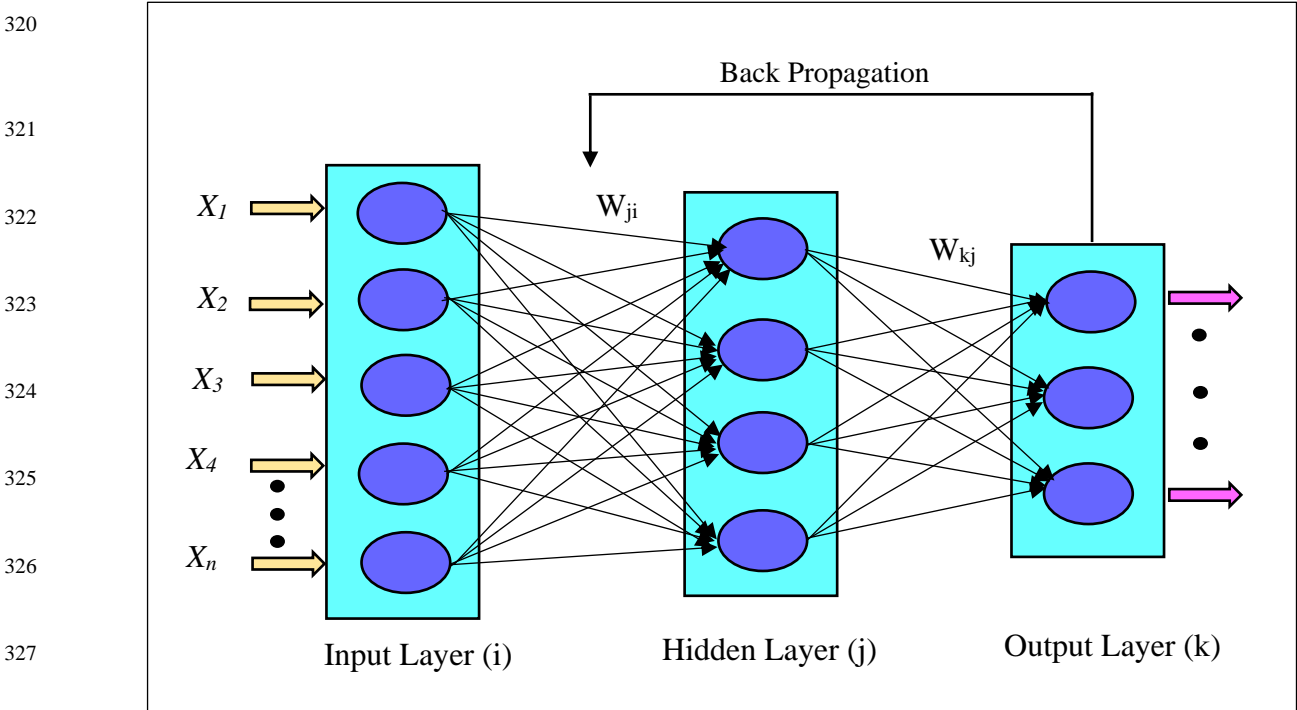
301 Fig. 11. Plots of DIs based on ACMSC for 10%, 15%, 20%, 25% and 30% damage at different
302 locations in the Mülheim-Kärlich cooling tower

305 **3.2 Damage quantification using Artificial Neural Network (ANN)**

306 **3.2.1 Background**

307 Artificial Neural Network (ANN) is a smart and efficient technique that is used to recognise
308 patterns, analyse data, and provide nonlinear control. It is capable of learning the solution to a problem
309 from the set of examples and also it has a high processing speed. The mechanism of the neural network
310 inspires from the biological nervous system. The neuron is the combination of body, axon, dendrites,
311 and synapses. In the biological network, dendrites (input) transfer the signals to the neurons, while
312 axon (output) carries away the signal from the neurons. Synapses are used to communicate between
313 neurons. Each synapse has its own strength which is similar to the weight used in the neural network
314 [23].

315 The concept of the neural network was introduced by McCulloch and Pitts in 1943 [24]. The
316 structure of the ANN is the combination of three layers which are the input layer, the output layer and
317 one or more hidden layers. Each layer has a number of processing units called neurons. All the inputs
318 are fed to the network through the input layer (i), which is the first layer of ANN, as shown in Fig. 12,
319 while the last layer, which is called the output layer (k), gives the outputs.



328 Fig. 12: Neural network architecture

329

330

331

332

333

334

335

336

337

338

339

340

341

342

343

344

345

346

347

348

349

350

351

A single neuron is a nonlinear function that transforms a set of input variables into output variables. The transformation process of the McCulloch and Pitts model can be presented, as shown in Equation 3. The input variables (x_i) are multiplied by the weights (w_{ji}) and then added to all the other weighted input variables to give a total input to a resultant unit. In Equation 3 w_{j0} is the bias which corresponds to the firing threshold in a biological neuron. The net input value in the hidden layer (z_i) is processed using linear or nonlinear activation function (g) as shown in Equation 4. The output from the hidden layer (z_j) is considered as the input of the output layer. The final output (z_k) can be written, as shown in Equation 5.

$$z_i(x) = \sum_{i=1}^n w_{ji}x_i + w_{j0} \quad (3)$$

$$z_j(x) = g\left(\sum_{i=1}^n w_{ji}x_i + w_{j0}\right) \quad (4)$$

$$z_k(x) = g\left(\sum_{j=1}^m w_{kj} g\left(\sum_{i=1}^n w_{ji}x_i + w_{j0}\right) + w_{k0}\right) \quad (5)$$

Neural network training is performed by changing the weights and bias parameters to obtain the predefined targets (t_k). The total error (E) can be calculated from the average squared difference between outputs and targets, as shown in Equation 6.

$$E = \frac{1}{2} \sum_{k=1}^m (t_k - z_k(x))^2 \quad (6)$$

A feed-forward neural network having one hidden layer with the backpropagation learning technique is used to train the network in the present study. This feed-forward network consists of three layers which include input, hidden and output layers. The network input is connected to the first layer and each subsequent layer is connected to the one before it. The final layer produces the output of the network. Feed-forward networks are the ones in which the information moves through layers in only one direction, i.e., from the input layer to the output layer through hidden layers. Backpropagation belongs to supervised learning, which used the known behaviour to train the network. The error term

352 is backpropagated to alter the weights and the bias to obtain the optimum network, as shown in Fig.
353 12 [25]. It is necessary for a network to have adequate training.

354 In the present study, ANN was developed to predict the damage severity in a hyperbolic cooling
355 tower. The absolute changes in mode shape curvature (ACMSC) based damage index was used as the
356 input for the ANN network instead of mode shape values to avoid overfitting and reduce the
357 computational effort. Also, lessor data can be used for input of the network to train the network.

358 The selection of ANN architecture is mainly based on trial and error because there is no
359 theoretical procedure [26]. Neural network architecture consists of different key features such as type
360 of neural network, number of hidden layers, number of hidden neurons, learning algorithms, transfer
361 functions and convergence algorithm.

362 This paper used the multilayer feed forward network with backpropagation algorithm in
363 MATLAB 2018a to learn the relationship between inputs and outputs. The number of hidden layers
364 and the number of hidden neurons depend on the complexity of the problem and the amount of noise
365 [27]. Insufficient selection of hidden layers will cause large training and generalisation errors. The
366 selection of the convergence algorithm depends on the complexity, size of the training set and the
367 number of input parameters in the neural network. Convergence algorithm has different performance
368 speed, memory requirements and different efficiencies. In this paper, optimum convergence was
369 achieved by using Bayesian Regularization (trainbr) as a training algorithm. This algorithm typically
370 requires more time to train, but it gives good generalization for complicated, limited, or noisy data
371 sets. Regularization method [28], early stopping method [29] and Pruning [30] are the few methods
372 which can be used to minimise overfitting and increase the generalization capacity of the training
373 network. The training function (trainbr) usually works well with the early stopping method and hence
374 in this paper, the early stopping method [31], which is also easy to handle, is used to terminate the
375 training process. The termination of the training process was done manually.

376

377 3.2.2 Data extraction from numerical model

378 Mülheim-Kärlich cooling tower in Germany mentioned earlier was studied for damage assessment
379 using ANN. A validated FEM model of this cooling tower was used to create the input data for ANN.
380 Capability of detecting and locating damage in the Mülheim-Kärlich cooling tower using the DIs based
381 on ACMSC has been presented in section 2.1.

382 This time damage is simulated by reducing the Young's modulus in 20 different locations along the
383 height of the cooling tower for a range of damage severities (5%, 10%, 15%, 17%, 20%, 24%, 25%,
384 28%, 30%, 50%). Mode shape data are extracted from the intact and damaged structures using the
385 validated FE model. Mode shape data generated from the FEMs are free from noise. But in practice
386 vibration responses of the structure are polluted with environmental and measurement noise.
387 Therefore, field testing conditions are simulated by adding white Gaussian noise [32],[33] and with
388 limited data points. Adding noise not only reduces the overfitting but can also be used for faster
389 optimization. Adding artificial noise into the input data set is one way of improving the generalization
390 error, and it also improves the robustness of the model [34]–[36]. Moreover, adding noise also expands
391 the size of the data set, which is used for training. Equation 7 [33] was used to create noise-
392 contaminated mode shape data by changing the random noise level (ρ_x^ϕ) by 2%, 5%, 10%, 15% and
393 20%.

$$394 \quad \overline{\phi}_{xi} = \phi_{xi}(\mathbf{1} + \gamma_x^\phi \rho_x^\phi |\phi_{max,i}|) \quad (7)$$

395 In the above equation, $\overline{\phi}_{xi}$ and ϕ_{xi} denote the mode shape values with and without noise at the
396 location of x in the i^{th} mode. γ_x^ϕ is a random number with a variance equal to 1 and mean equal to zero.
397 $|\phi_{(max,i)}|$ denotes the absolute maximum mode shape value.

398

399 3.2.3 ANN model architecture

400 All the extracted mode shape data are converted to DIs using Equation 2 to create the input data for
401 the neural network. Damage severity and location are used as the target values for the neural network.

402 Altogether 612 data samples are used to train the network. A higher number of input data will increase
403 the accuracy of the outcome. The number of input and output nodes depends on the number of variables
404 in input and output data sets. A trial and error process was used to find the number of neurons in the
405 hidden layer. After finding the best network configuration, few trials were carried out to acquire the
406 best network with minimum error. This was been done because each network assigns different weights
407 and sampling, which will create different networks. The input data is divided into three sets, namely
408 training (75%), testing (20%) and validation (5%). Training data set is used during the training to
409 adjust its error while the validation set is used to measure network generalization. Testing data set has
410 no effects on training, but they are used to measure the performance of the network during and after
411 training.

412 The neural network shown in Fig. 13 has one hidden layer which contains 24 hidden neurons. Letters
413 'w' and 'b' refer to the weight and bias, respectively. The training function of the network is Bayesian
414 Regularization (trainbr), while the transfer function of the hidden layer is the hyperbolic tangent
415 sigmoid function. Performance of the trained neural network can be evaluated using mean square error
416 (MSE) and regression analysis. Regression plots of trained neural network are presented in Fig.14 in
417 which the regression value (R) represents the correlation between output and targets. The value close
418 to 1 means, it has a close relationship while 0 means random relationship. The overall values of R
419 (0.99274) confirm that the network is properly trained. These graphs illustrate the variation of target
420 values (FEM results) vs ANN outputs. As shown in Fig.14, the best fit line of the trained network
421 overlaps with perfect fit line ($Y=T$). MSE is the average squared difference between outputs and
422 targets. MSE value of this trained network is 0.0289. Moreover, the error histogram Fig. 15, shows the
423 variation of error between targets and outputs for training and testing stages of NN. In most instances
424 these are at zero line.

425
426
427
428
429
430
431
432
433
434
435
436
437
438
439
440
441
442
443
444
445
446
447
448
449
450
451
452
453
454
455
456

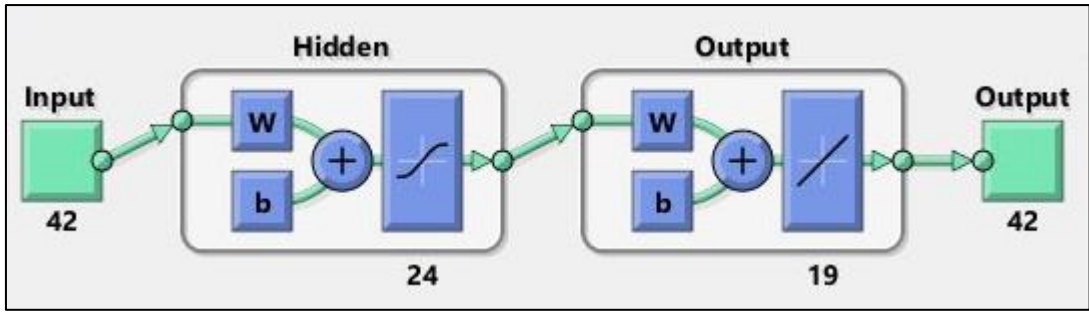


Fig. 13. Neural network configuration

Once the network is trained, it can be used to predict the location of damage and the severity of the damage in unknown scenarios.

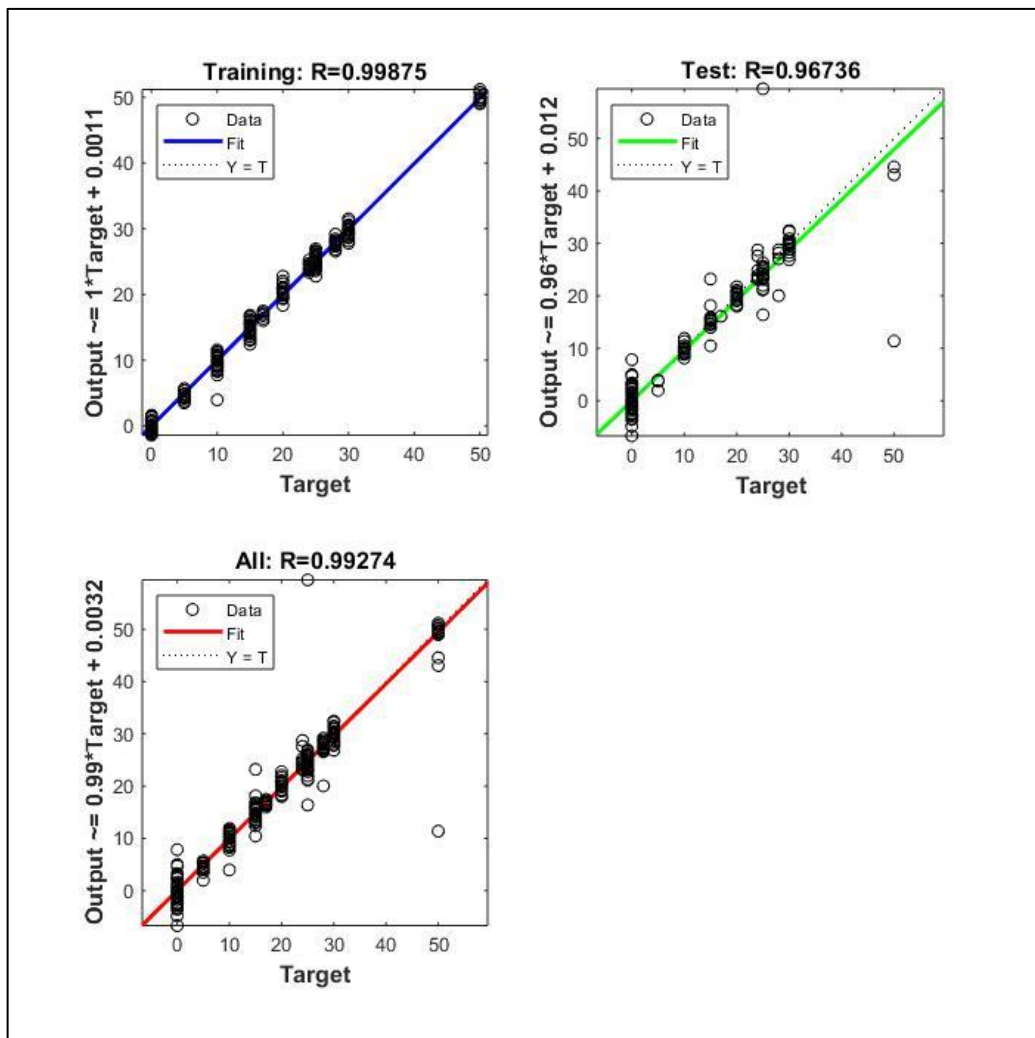
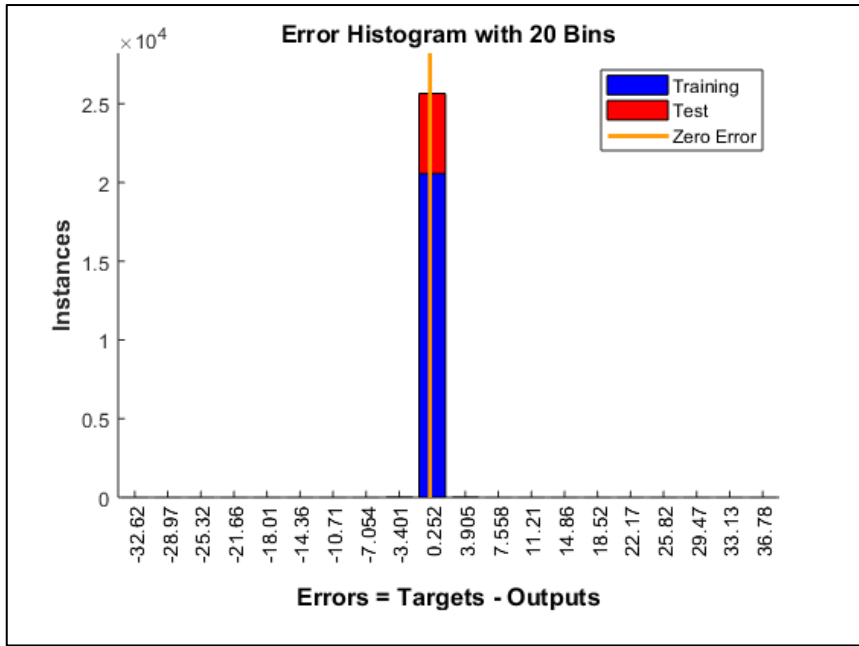


Fig. 14. Regression plots of trained Neural Network

457
458
459
460
461
462
463
464
465
466
467
468



469

Fig. 15. Error histogram

470

4. Results and Discussion

471

4.1 Single Damage Scenarios

472

The developed ANN is used to predict the location and severity in unknown damage cases. Seventy-

473

five damage cases corresponding to 12 locations, 12 severities and 10 noise levels are simulated in the

474

FEM of Mülheim-Kärlich cooling tower and mode shape data corresponding to each damage case are

475

extracted. As the next step, DI values of unknown damage cases are calculated using Equation 2. These

476

DIs are fed into the trained neural network in order to test its ability to locate and quantify damage.

477

The capability of the network is tested considering five types of unknown damage cases as follows.

478

(i) DIs calculated from different damage severities under different noise conditions

479

(ii) DIs calculated from different damage severities at different locations with respect to height and

480

circumference at that height

481

(iii) DIs calculated from different damage severities with the same noise

482

(iv) DIs calculated for same damage severity, but with different noise conditions

483

(v) DIs calculated for zero damage severity

484 *4.1.1 DIs calculated from different damage severities under different noise conditions*

485 Each of these damage scenarios are different, and none of these damage severities and noise
 486 conditions were used to train the network. Table 3 shows the damage cases tested on the trained neural
 487 network with actual damage severities and neural network predictions. It can be seen that the variation
 488 between two actual and predicted severities (in columns 3 and 5) is less than 2.2%. This confirms that
 489 the trained neural network (NN) is capable of accurately predicted different damage severities even
 490 under different noise conditions. Figs 16 (a), (b), (c), and (d) show the graphical representation of few
 491 cases in Table 3. It can be seen that the actual and predicted damage severities match reasonably well.

492 Table 3. Neural network predictions for different damage severities with different noise conditions
 493

Damage case	Actual Damage			NN Prediction		Variation
	Noise	Severity	Location	Severity	Location	
1	0%	13%	H _i =30.79 m	13.18%	H _i =30.79 m	-0.18%
2	0%	13%	H _i =133 m	12.92%	H _i =133 m	0.08%
3	0%	33%	H _i =153.2 m	32.88%	H _i =153.2 m	0.12%
4	0%	33%	H _i =93.27 m	33.37%	H _i =93.27 m	-0.37%
5	0%	40%	H _i =153.2 m	40.83%	H _i =153.2 m	-0.83%
6	0%	55%	H _i =125 m	54.39%	H _i =125 m	0.61%
7	3%	13%	H _i =30.79 m	13.73%	H _i =30.79 m	-0.73%
8	3%	13%	H _i =93.27 m	13.59%	H _i =93.27 m	-0.59%
9	3%	13%	H _i =153.2 m	13.66%	H _i =153.2 m	-0.66%
10	3%	40%	H _i =93.27 m	40.51%	H _i =93.27 m	-0.51%
11	4%	13%	H _i =30.79 m	14.27%	H _i =30.79 m	-1.27%
12	4%	33%	H _i =93.27 m	33.17%	H _i =93.27 m	-0.17%
13	4%	33%	H _i =133 m	32.53%	H _i =133 m	0.47%
14	7%	13%	H _i =93.27 m	12.52%	H _i =93.27 m	0.48%
15	7%	33%	H _i =30.79 m	33.18%	H _i =30.79 m	-0.18%
16	7%	40%	H _i =93.27 m	42.16%	H _i =93.27 m	-2.16%
17	12%	13%	H _i =30.79 m	13.01%	H _i =30.79 m	-0.01%
18	12%	13%	H _i =93.27 m	13.67%	H _i =93.27 m	-0.67%
19	12%	33%	H _i =30.79 m	32.78%	H _i =30.79 m	0.22%

20	12%	33%	$H_i=93.27$ m	33.34%	$H_i=93.27$ m	-0.34%
21	12%	40%	$H_i=93.27$ m	41.47%	$H_i=93.27$ m	-1.47%
22	12%	55%	$H_i=125$ m	56.58%	$H_i=125$ m	-1.58%

494

495

496

497

498

499

500

501

502

503

504

505

506

507

508

509

510

511

512

513

514

515

516

517

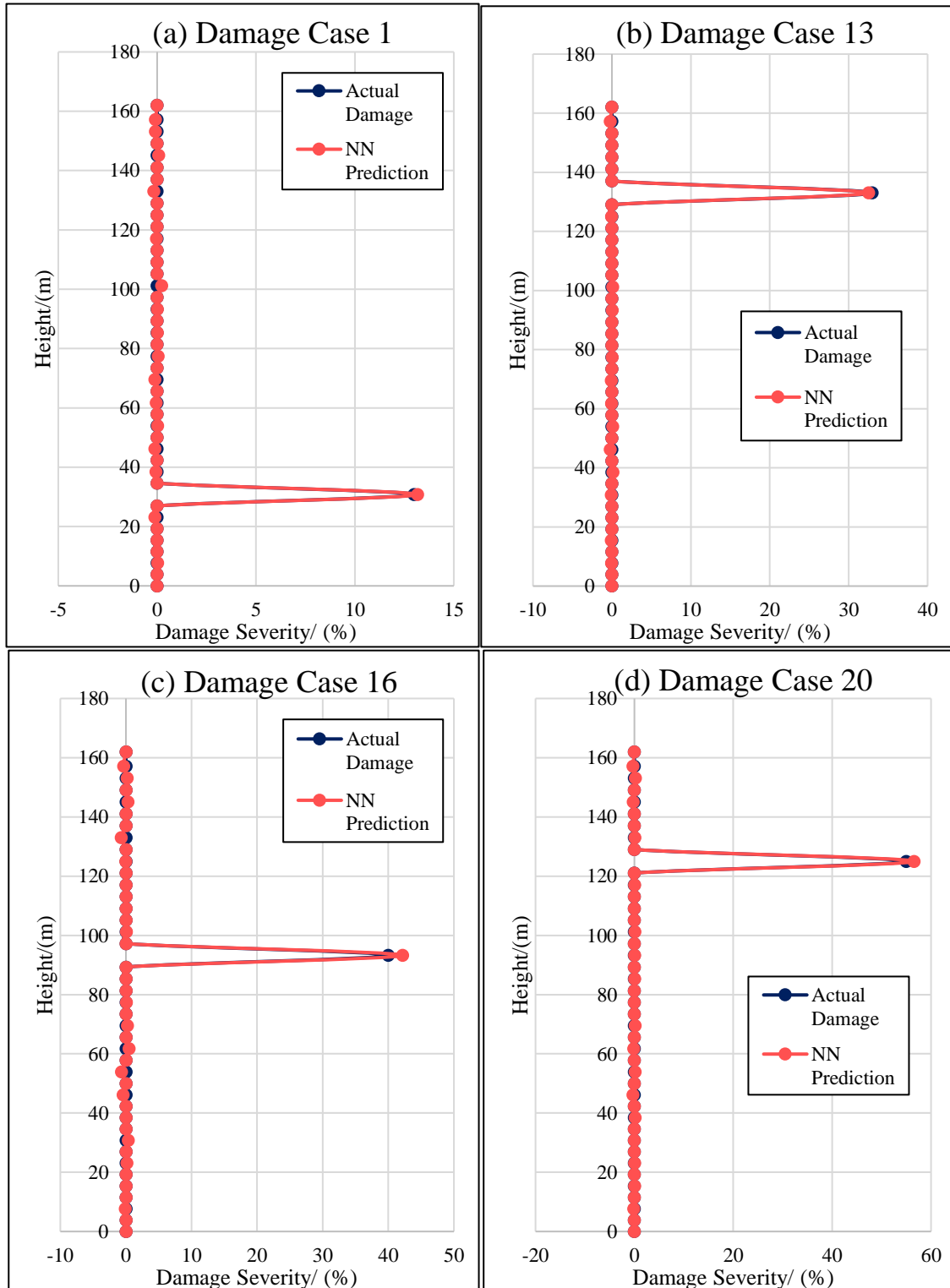
518

519

520

521

522



523

Fig. 16. Graphical representation of few damage cases in Table 3

524 *4.1.2 DIs calculated from different damage severities at different locations with respect to height*
 525 *and circumference at that height*

526 In order to test the ability of the trained neural network, unknown damage severity cases at different
 527 locations with respect to height and circumference at that height are considered, as shown in Table 4.
 528 These damage locations and severity cases are completely random. It can be seen that the variation
 529 between the actual and predicted severities (in columns 3 and 5) is less than 2.4 %. This verifies that
 530 the trained NN is capable of determining other damage severities and at other locations different from
 531 that used in the training.

532 Table 4. Neural network outcomes for different damage severity with different Locations

Damage case	Absolute Damage			NN outcome		Variation
	Noise	Severity	Location	Severity	Location	
1	0%	52%	Hi=92.8 m	54.4%	Hi=93.2 m	-2.4 %
2	0%	23%	Hi=69.55 m	23.8%	Hi=69.55 m	-0.8 %
3	0%	45%	Hi=125 m	45.8%	Hi=125 m	-0.8 %
4	3%	18%	Hi=46.8m	16.44%	Hi=46.2 m	1.56 %
5	3%	23%	Hi=69.55m	22.15%	Hi=69.55 m	0.85 %
6	4%	52%	Hi=92.8m	52.7%	Hi=93.2 m	-0.7 %
7	4%	23%	Hi=124.2m	20.7%	Hi=125 m	2.3 %
8	7%	18%	Hi=46.8m	18.6%	Hi=46.2m	-0.6 %
9	7%	45%	Hi=125m	44.72%	Hi=125m	0.28 %
10	7%	23%	Hi=69.55m	23.17%	Hi=69.55m	-0.17%

533
 534 *4.1.3 DIs calculated from different damage severities with same noise conditions*
 535

536 In order to test the ability of the trained neural network, unknown damage severity cases with the
 537 same noise conditions are tested, as shown in Table 5. These damage severity cases are completely
 538 random. Same noise conditions which are used to train the network are used to train the network. It
 539 can be seen that the variation between the actual and predicted severities (in columns 3 and 5) is less

540 than 2.2%. This verifies that the trained NN is capable of determining new damage severities even
 541 under the same noise conditions.

542 Table 5. Neural network outcomes for different damage severities with same noise conditions

Damage case	Absolute Damage			NN outcome		Variation
	Noise	Severity	Location	Severity	Location	
1	0%	12.5%	H _i =61.73 m	11.72%	H _i =61.73 m	0.78%
2	0%	12.5%	H _i =145.1 m	11.87%	H _i =145.1 m	0.63%
3	0%	22.5%	H _i =125 m	22.24%	H _i =125 m	0.26%
4	0%	35%	H _i =125 m	35.12%	H _i =125 m	-0.12%
5	2%	12.5%	H _i =61.73 m	12.40%	H _i =61.73 m	0.1%
6	2%	22.5%	H _i =145.1 m	22.2%	H _i =145.1 m	0.30%
7	2%	22.5%	H _i =61.73 m	22.18%	H _i =61.73 m	0.32%
8	2%	35%	H _i =125 m	34.24%	H _i =125 m	0.76%
9	5%	12.5%	H _i =145.1 m	12.57%	H _i =145.1 m	-0.07%
10	5%	22.5%	H _i =61.73 m	22.92%	H _i =61.73 m	-0.42%
11	5%	35%	H _i =125 m	36.20%	H _i =125 m	-1.20%
12	5%	35%	H _i =145.1 m	33.60%	H _i =145.1 m	1.40%
13	10%	12.5%	H _i =61.73 m	13.26%	H _i =61.73 m	-0.76%
14	10%	12.5%	H _i =125 m	14.67%	H _i =125 m	-2.17%
15	10%	22.5%	H _i =145.1 m	22.76%	H _i =145.1 m	-0.26%
16	10%	35%	H _i =145.1 m	35.87%	H _i =145.1 m	-0.87%
17	15%	12.5%	H _i =61.73 m	12.44%	H _i =61.73 m	0.06%
18	15%	12.5%	H _i =145.1 m	12.24%	H _i =145.1 m	0.26%
19	15%	22.5%	H _i =125 m	24.54%	H _i =125 m	-2.04%
20	15%	35%	H _i =145.1 m	35.65%	H _i =145.1 m	-0.65%
21	20%	12.5%	H _i =125 m	11.31%	H _i =125 m	1.19%
22	20%	12.5%	H _i =61.73 m	12.36%	H _i =61.73 m	0.16%
23	20%	22.5%	H _i =125 m	24.37%	H _i =125 m	-1.87%
24	20%	35%	H _i =145.1 m	33.36%	H _i =145.1 m	1.64%

543

544 *4.1.4 DIs calculated from same damage severity, but with different noise conditions*

545 The capability of locating and quantifying damages in the cooling tower is also tested for the same
 546 damage severity (which was used for training the network), but under different noise conditions.
 547 Results are shown in Table 6, where the variation in percentage severity between actual predicted
 548 values (in columns 3 and 5) is less than 1.75%. This trained neural network is therefore capable of
 549 detecting damage severity even in the presence of different noise conditions.

550 Table 6. Neural network outcomes for same damage severity, but with different noise conditions

Damage case	Absolute Damage			NN outcome		Variation
	Noise	Severity	Location	Severity	Location	
1	3%	5%	Hi=30.79 m	4.43%	Hi=30.79 m	0.56%
2	3%	5%	Hi= 153.2 m	4.99%	Hi= 153.2 m	0.01%
3	3%	24%	Hi=93.27 m	22.26%	Hi=93.27 m	1.74%
4	3%	24%	Hi=133 m	25.55%	Hi=133 m	-1.55%
5	4%	5%	Hi=30.79 m	4.37%	Hi=30.79 m	0.63%
6	4%	5%	Hi=93.27 m	5.23%	Hi=93.27 m	-0.23%
7	4%	24%	Hi=133 m	25.53%	Hi=133 m	-1.53%
8	4%	24%	Hi= 30.79 m	25.35%	Hi= 30.79 m	-1.35%
9	7%	5%	Hi=30.79 m	5.04%	Hi=30.79 m	-0.04%
10	7%	5%	Hi=93.27 m	5.01%	Hi=93.27 m	-0.01%
11	7%	24%	Hi=133 m	22.59%	Hi=133 m	1.41%
12	7%	24%	Hi= 153.2 m	23.25%	Hi= 153.2 m	0.75%
13	12%	5%	Hi=30.79 m	5.35%	Hi=30.79 m	-0.35%
14	12%	5%	Hi= 153.2 m	4.90%	Hi= 153.2 m	0.10%
15	12%	24%	Hi=93.27 m	24.68%	Hi=93.27 m	-0.68%
16	12%	24%	Hi= 133 m	24.92%	Hi= 133 m	-0.92%

551
552
553 *4.1.5 DIs calculated from zero damage severity*

554 The trained artificial neural network is tested using the DIs calculated from locations where the
 555 damage does not exist (zero damage severity). The results are presented in Table 7. The variation of

556 percentage severity between actual and predicted values is less than 0.15%. This trained neural network
557 therefore will not capture false alarms.

558 Table 7. Neural network outcome for zero damage severities

Damage case	Location	Actual Damage	NN outcome	Variation
		Severity		
1	Hi=46.17 m	0%	0.11%	-0.11%
2	Hi=30.79 m	0%	-0.08%	0.08%
3	Hi=30.79 m	0%	0.15%	-0.15%

559

560 **Conclusions**

561 Hyperbolic cooling towers are large, reinforced concrete structures used to cool wastewater. Though
562 they are designed to have long lives, damage can occur due to one of many reasons. Such damage must
563 be detected and assessed at the outset to enable appropriate retrofitting and prevent the collapse of
564 these large structures. Due to their unique shape, hyperbolic cooling towers have rather complex
565 vibration characteristics. Traditional vibration-based methods are hence not applicable to detect, locate
566 and quantify damage in them. This paper developed and presented a method incorporating artificial
567 neural networks together with the absolute change in mode shape curvature-based DIs for locating and
568 quantifying damages in hyperbolic cooling towers. The proposed method includes the input data using
569 absolute mode shape curvature method, network architecture, network training and validation
570 processes. The feasibility of the trained neural network was illustrated through its application to several
571 damage scenarios, even in the presence of noise polluted data. Results confirm the accuracy of the
572 proposed method. The outcome of this paper will help towards the safe efficient functioning of
573 hyperbolic cooling towers.

574 **Acknowledgments**

575 The first author acknowledges with appreciation for the continuous supervision provided by the
576 supervisors, the immense assistance for experiments provided by Dr Khac Duy Nguyen, Dr S.

577 Aghdamy, Design and Manufacturing Centre at QUT, QUT pilot plant at Banyo and the support for
578 this research provided by QUT postgraduate research scholarship.

579 *The raw data required to reproduce these findings cannot be shared at this moment as these data*
580 *also forms a part of ongoing research*

581 **References**

- 582 [1] P. L. Gould and W. B. Krätzig, *Cooling tower structures*. Boca Raton: CRC Press LLC, 1998.
- 583 [2] E. Asadzadeh and M. Alam, “A Survey on Hyperbolic Cooling Towers,” *Int. J. Civil, Archit.*
584 *Struct. Constr. Eng.*, vol. 8, pp. 1022–1034, Dec. 2014.
- 585 [3] H.-J. Park, K.-Y. Koo, and C.-B. Yun, “Modal flexibility-based damage detection technique of
586 steel beam by dynamic strain measurements using FBG sensors,” *Steel Struct.*, vol. 7, pp. 11–
587 18, 2007.
- 588 [4] A. Zingoni, “Structural health monitoring, damage detection and long-term performance,” *Eng.*
589 *Struct.*, vol. 12, no. 27, pp. 1713–1714, 2005.
- 590 [5] S. W. Doebling and C. R. Farrar, “Computation of structural flexibility for bridge health
591 monitoring using ambient modal data,” 1996.
- 592 [6] M. M. F. Yuen, “A numerical study of the eigenparameters of a damaged cantilever,” *J. Sound*
593 *Vib.*, vol. 103, no. 3, pp. 301–310, 1985, doi: [https://doi.org/10.1016/0022-460X\(85\)90423-7](https://doi.org/10.1016/0022-460X(85)90423-7).
- 594 [7] T. M. Whalen, “The behavior of higher order mode shape derivatives in damaged, beam-like
595 structures,” *J. Sound Vib.*, vol. 309, no. 3–5, pp. 426–464, 2008.
- 596 [8] H. Abdul Razak and Z. Ismail, “Flexural Stiffness Determination Using Mode Shape
597 Derivative,” *Asian J. Civ. Eng. (Building Housing)*, vol. 3, Jan. 2006.
- 598 [9] S. M. C. M. Randiligama, D. P. Thambiratnam, T. H. T. Chan, S. Fawzia, and K. Duy Nguyen,
599 “Vibration based damage detection in hyperbolic cooling towers using coupled method,” *Eng.*
600 *Fail. Anal.*, vol. 121, p. 105156, 2021, doi: <https://doi.org/10.1016/j.engfailanal.2020.105156>.
- 601 [10] Z. Y. Shi, S. S. Law, and L. M. Zhang, “Improved damage quantification from elemental modal
602 strain energy change,” *J. Eng. Mech.*, vol. 128, no. 5, pp. 521–529, 2002.

- 603 [11] C. Mares and C. Surace, "An application of genetic algorithms to identify damage in elastic
604 structures," *J. Sound Vib.*, vol. 195, no. 2, pp. 195–215, 1996.
- 605 [12] Z. X. Tan, D. P. Thambiratnam, T. H. T. Chan, M. Gordan, and H. Abdul Razak, "Damage
606 detection in steel-concrete composite bridge using vibration characteristics and artificial neural
607 network," *Struct. Infrastruct. Eng.*, vol. 16, no. 9, pp. 1247–1261, 2020.
- 608 [13] N. Jayasundara, D. P. Thambiratnam, T. H. T. Chan, and A. Nguyen, "Damage detection and
609 quantification in deck type arch bridges using vibration based methods and artificial neural
610 networks," *Eng. Fail. Anal.*, vol. 109, p. 104265, 2020.
- 611 [14] X. Wu, J. Ghaboussi, and J. H. Garrett Jr, "Use of neural networks in detection of structural
612 damage," *Comput. Struct.*, vol. 42, no. 4, pp. 649–659, 1992.
- 613 [15] A. M. A. Alzawi, "Vibration isolation using in-filled geofom trench barriers," 2011.
- 614 [16] R. P. Bandara, T. H. T. Chan, and D. P. Thambiratnam, "Structural damage detection method
615 using frequency response functions," *Struct. Heal. Monit.*, vol. 13, no. 4, pp. 418–429, 2014.
- 616 [17] A. K. Pandey, M. Biswas, and M. M. Samman, "Damage detection from changes in curvature
617 mode shapes," *J. Sound Vib.*, vol. 145, no. 2, pp. 321–332, 1991.
- 618 [18] W. B. KRÄTZIG, "Giga-Shells for Energy Generation: Natural Draft Cooling Towers and Solar
619 Updraft Chimneys." Proc. ISCT, 2012.
- 620 [19] A. M. Nasir, D. P. Thambiratnam, D. Butler, and P. Austin, "Dynamics of axisymmetric
621 hyperbolic shell structures," *Thin-walled Struct.*, vol. 40, no. 7–8, pp. 665–690, 2002.
- 622 [20] A. Rytter, "Vibrational based inspection of civil engineering structures." Dept. of Building
623 Technology and Structural Engineering, Aalborg University, 1993.
- 624 [21] S. J. S. Hakim and H. A. Razak, "Damage detection of steel bridge girder using artificial neural
625 networks," *Emerg. Technol. Non-Destructive Test. V*, vol. 409, 2012.
- 626 [22] K.-D. Nguyen, T. H. T. Chan, and D. P. Thambiratnam, "Structural damage identification based
627 on change in geometric modal strain energy–eigenvalue ratio," *Smart Mater. Struct.*, vol. 25,
628 no. 7, p. 75032, 2016.
- 629 [23] C. M. Bishop, "Neural networks and their applications," *Rev. Sci. Instrum.*, vol. 65, no. 6, pp.

630

1803–1832, 1994.

631

[24] W. S. McCulloch and W. Pitts, “A logical calculus of the ideas immanent in nervous activity,” *Bull. Math. Biophys.*, vol. 5, no. 4, pp. 115–133, 1943.

632

633

[25] Y. H. Zweiri, J. F. Whidborne, and L. D. Seneviratne, “A three-term backpropagation algorithm,” *Neurocomputing*, vol. 50, pp. 305–318, 2003.

634

635

[26] R. P. Bandara, T. H. T. Chan, and D. P. Thambiratnam, “Frequency response function based damage identification using principal component analysis and pattern recognition technique,” *Eng. Struct.*, vol. 66, pp. 116–128, 2014.

636

637

638

[27] U. Dackermann, “Vibration-based damage identification methods for civil engineering structures using artificial neural networks.” 2009.

639

640

[28] A. Krogh and J. Vedelsby, “Neural network ensembles, cross validation, and active learning,” in *Advances in neural information processing systems*, 1995, pp. 231–238.

641

642

[29] L. Prechelt, “Automatic early stopping using cross validation: quantifying the criteria,” *Neural Networks*, vol. 11, no. 4, pp. 761–767, 1998.

643

644

[30] B. Hassibi and D. Stork, “Second order derivatives for network pruning: Optimal brain surgeon,” *Adv. Neural Inf. Process. Syst.*, vol. 5, pp. 164–171, 1992.

645

646

[31] E. Sariev and G. Germano, “Bayesian regularized artificial neural networks for the estimation of the probability of default,” *Quant. Financ.*, vol. 20, no. 2, pp. 311–328, Feb. 2020, doi: 10.1080/14697688.2019.1633014.

647

648

649

[32] B. Lukić, D. Saletti, and P. Forquin, “Use of simulated experiments for material characterization of brittle materials subjected to high strain rate dynamic tension,” *Philos. Trans. R. Soc. A Math. Phys. Eng. Sci.*, vol. 375, no. 2085, p. 20160168, 2017.

650

651

652

[33] Z. Y. Shi, S. S. Law, and L. M. Zhang, “Damage localization by directly using incomplete mode shapes,” *J. Eng. Mech.*, vol. 126, no. 6, pp. 656–660, 2000.

653

654

[34] C. M. Bishop, “Training with noise is equivalent to Tikhonov regularization,” *Neural Comput.*, vol. 7, no. 1, pp. 108–116, 1995.

655

656

[35] C. M. Bishop, *Neural networks for pattern recognition*. Oxford university press, 1995.

657 [36] R. Reed and R. J. MarksII, *Neural smithing: supervised learning in feedforward artificial neural*
658 *networks*. Mit Press, 1999.

659